THE JOURNAL OF PHYSICAL CHEMISTRY C

Article

pubs.acs.org/JPCC

Formation of Stabilized Ketene Intermediates in the Reaction of O(^{3}P) with Oligo(phenylene ethynylene) Thiolate Self-Assembled Monolayers on Au(111)

Wenxin Li, Grant G. Langlois, Natalie A. Kautz, and S. J. Sibener*

The James Franck Institute and Department of Chemistry, The University of Chicago, 929 E 57th Street, Chicago, Illinois 60637, United States

ABSTRACT: We have taken steps to develop a methodology for quantifying the kinetics and dynamics of bimolecular reactions through spectroscopic monitoring of reactants and products during exposure of well-ordered self-assembled monolayers (SAMs) to supersonic beams of atomic reagents. The use of a SAM stabilizes highly energetic intermediates formed from bimolecular reactions at the vacuum/film interface due to rapid thermal equilibration with the SAM matrix that are otherwise not readily observed under single-collision conditions in the gas phase. In this paper, we will discuss the elucidation of the mechanistic details for the fundamental reaction between O(^{3}P) and phenyl-substituted alkyne bonds by monitoring chemical and structural changes in an oligo(phenylene ethynylene) SAM reacting with O(^{3}P) under collision conditions having specified initial reaction orientation. Utilizing time-resolved reflection−absorption infrared spectroscopy (RAIRS) and scanning tunneling microscopy (STM) under ultrahigh vacuum conditions, we have confirmed electrophilic addition of O(^{3}P) onto the alkyne moieties, resulting in formation of a ketene intermediate via phenyl migration. Under single-collision conditions in the gas phase, the vibrationally excited ketene intermediate cleaves to release CO. In contrast to this, formation of the condensed-phase stabilized singlet ketene is observed using RAIRS. Moreover, we have observed that the phenyl ring at the vacuum/film interface significantly cants toward the substrate plane as a result of this reaction. STM images of the SAM taken before and after O(^{3}P) exposure show an expansion of the ordered lattice resulting from formation of the new nonlinear molecular structures within the SAM, and the reaction preferentially propagates along the lattice direction of the monolayer domain. This approach of using preoriented reactive molecules in ordered SAMs in combination with angle- and velocity-selected energetic reagents provides a general approach for probing geometric constraints associated with reaction dynamics for a wide range of chemical reactions.

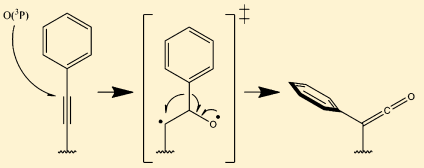

INTRODUCTION

At the heart of chemistry lies an initiative to both elucidate and predict the behavior of chemical reactions through analysis of the complex molecular dynamics taking place. However, direct study of reaction mechanisms is naturally precluded by establishment of some degree of control over the intended pathways. Historically, this has been accomplished in the gas phase through either excitation of relevant internal states of reacting molecules[1−4] or controlling their mutual orientation.[5] Early examples in the literature of the latter method include alignment of polar molecules in molecular beams using either hexapole or "brute-force" techniques.[6,7]

Our goal is to apply this same notion of stereodynamic control by dosing reactive species prepared in a molecular beam to the exposed interface of a self-assembled monolayer (SAM). SAMs offer unique opportunities to probe the mechanisms of reactions at interfaces due to their well-defined, ordered structures and chemical stability, and organothiolates on gold are a classically robust system of choice for studying reactions of organic matter.[8] Their self-assembly in solution is often simple and effective, utilizing precursors with nearly any functional terminus of choice.[9,10] The use of a SAM surface as an ensemble of reactants is also advantageous due to its ability to rapidly dissipate excess energy.[11−13] Highly energetic intermediates that fall apart or further react in the gas phase can instead be stabilized at the interface, a process akin to collisional stabilization in the gas phase at high pressures. Utilizing reflective spectroscopic techniques and high-resolution scanning probe microscopy, we are uniquely situated to successfully characterize reactions occurring at these interfaces in both real time and real space.

We aim to directly observe reaction products in the foundational reactions of O(^{3}P) with unsaturated hydrocarbons using this technique, specifically considering addition onto phenyl-substituted alkynes. Reactions with phenylacetylene, 2-propynylbenzene, and biphenylacetylene have previously been experimentally characterized, with energetic barriers associated with O(^{3}P) addition onto the side chains measured to be low (<8 kJ/mol) compared with the phenyl rings (~20 kJ/mol).[14,15] Specifically in the case of biphenylacetylene, Eichholtz et al. reported the formation of biphenyl as a main product and proposed a mechanism for its formation through, in part, decomposition of a vibrationally excited biphenylketene intermediate via phenyl ring migration to release CO.[15] This

Received: May 6, 2014
Revised: July 1, 2014
Published: July 11, 2014

   dx.doi.org/10.1021/jp504466r | J. Phys. Chem. C 2014, 118, 15846−15852

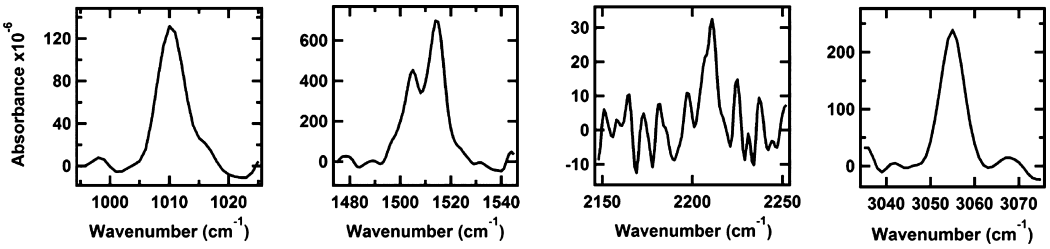

Figure 1. Relevant vibrational modes of prepared oPE-SAM as measure by RAIRS: (from left to right) C—C bending mode at 1010 cm^{-1}, C═C semicircle stretches at 1504 and 1514 cm^{-1}, alkyne stretching mode at 2210 cm^{-1}, and C—H stretching mode at 3055 cm^{-1}. All modes are parallel to the molecular axis.

mechanism is supported by experimental[16−18] and theoretical[19−23] studies of analogous reactions with acetylene and other substituted alkynes where CO formation results from cleavage of singlet ketenes formed from intersystem crossing of long-lived triplet ketocarbenes. These observations are also in line with experimental studies of O(^{3}P) addition onto ethylene, where intersystem crossing is observed to contribute heavily to overall product formation.[24,25]

Ketenes have previously been directly observed in studies of acetylene/O(^{3}P) reactions in low-temperature solid matrices[26] and at high pressures,[27] so the ability to directly observe the biphenylketene intermediate expected in this reaction via rapid thermal equilibration of the reaction complex with the SAM matrix can be expected. The SAMs used in this study were composed of oligo(phenylene ethynylene)thiolate (oPE) molecules that have previously been shown to self-assemble onto Au(111) in solution to form well-ordered, densely packed monolayers of upright molecules.[28−30] This surface yields an exposed interface of phenyl-substituted alkyne bonds.

EXPERIMENTAL SECTION

SAM Preparation. oPE-SAMs were prepared on commercially fabricated Au(111) substrates deposited onto mica (1.1 cm × 1.0 cm), obtained from Agilent Technologies. These substrates were cleaned in a commercial UV/O_3 cleaning unit for 2 h, rinsed thoroughly with ethanol, and dried under a stream of pure nitrogen prior to immersion into a solution containing the oPE-SAM precursor.

A 2 mg amount of *S*-[4-[2-[4-(2-phenylethynyl)phenyl]-ethynyl]phenyl]thioacetate (oPE) and 25 μL of 30% (w/v) aqueous NH_3 (both obtained from Sigma−Aldrich) were diluted to 10 mL in a 2:1 acetone/ethanol mixture to form a 0.5 mM thiolate solution, similar to literature preparation.[31] A thioacetate precursor was used instead of the free thiol to prevent side reactions with functional groups in the SAM precursor backbone. Since SAMs formed from thioacetates are inferior in quality compared to those formed from free thiols,[32] the acetate protecting group is removed via base-catalyzed hydrolysis initiated by the addition of NH_3. The prepared solutions were left to sit at room temperature, with 30 min being sufficient for complete deprotection,[33] and the cleaned Au(111) substrates were immersed into these solutions for 24 h at 60 °C, followed by subsequent washes in fresh 2:1 acetone/ethanol and pure ethanol. This method routinely produces SAMs of high quality.[28,32]

Molecular Beam/Reflection−Absorption Infrared Spectroscopy. All reactions were carried out in a molecular beam scattering apparatus that consisted of an ultrahigh vacuum (UHV) chamber and supersonic molecular beam. Previous publications have described this instrument in great detail,[34] so only a brief description including the relevant modifications is included here.

A radio frequency plasma source was used to generate a supersonic atomic oxygen beam formed by igniting and expanding a gas mixture of 5% O_2 in neon through a water-cooled quartz nozzle. The beam is characterized using time-of-flight techniques to determine both the extent of O_2 dissociation and the average kinetic energy of the resultant O(^{3}P) atoms. Typical experimental conditions yield an O(^{3}P) flux of 9×10^{13} atoms/(cm^2 s), impinging upon SAM surfaces at normal incidence with an average kinetic energy of 9 kJ/mol. The energy was chosen to discourage side reactions, namely, the addition of O(^{3}P) onto the phenyl rings of oPE-SAM occurring near 18 kJ/mol.[15] Flux is determined from monitoring the change in pressure within the reaction chamber when it is open to the incoming beam, given that the extent of O_2 dissociation is known.

In situ time-resolved Fourier transform reflection−absorption infrared spectroscopy (RAIRS) is accomplished through the use of incoming infrared radiation from a commercial IR spectrometer (Nicolet 6700), which is polarized perpendicular to the substrate of interest prior to reflection at a 75° incidence angle and collected with a liquid-nitrogen-cooled MCT/A detector. Spectra were averages of 1000 scans at a 2 cm^{-1} resolution taken in reference to a clean Au(111)/mica substrate, with peaks fit to Gaussian line shapes with cubic polynomial baselines using a nonlinear least-squares routine. The time-resolved nature of this technique stems from the ability to block the incoming O(^{3}P) with the beam flag, allowing for precise control over the amount of time the SAM is exposed to incoming O(^{3}P).

UHV-Scanning Tunneling Microscopy. All scanning tunneling microscopy (STM) images were taken at room temperature in a commercial UHV-STM system (UHV 300 from RHK Technology, Inc.), with a base pressure of 1×10^{-10} Torr. Reacted SAMs were exposed to the molecular beam in the RAIRS system before transferring through air to the STM system, with total exposure to air lasting less than 10 min. STM images were taken with typical scanning parameters of ±0.7 V and 40−50 pA. Fresh oPE-SAM samples were prepared for each reacted surface imaged.

RESULTS

RAIRS signals detailed in Figure 1 show relevant example absorption bands of oPE-SAM on polycrystalline gold substrates, the locations of which are in good agreement with literature.[29] Because of the surface selection rule, only vibrational modes with dipole moments perpendicular to the surface are observable,[35] allowing inferences regarding molecular orientation to be made. The average tilt angle of the

dx.doi.org/10.1021/jp504466r | J. Phys. Chem. C 2014, 118, 15846−15852

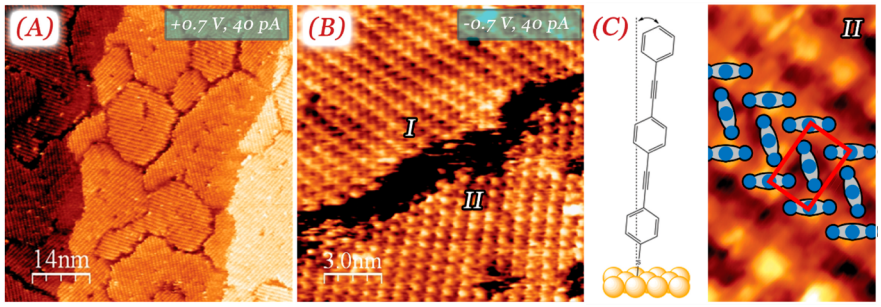

Figure 2. (A) oPE readily forms an ordered monolayer with large domains on Au(111) in solution. (B) The monolayer consists of two types of domains: a "commensurate" (I) and an "incommensurate" (II) structure, both of which have been observed previously in the literature. We observe that the overall structure of the monolayer is dominated (~75%) by the "incommensurate" domains. (C) The oPE molecules are anchored with their molecular axes nearly perpendicular to the Au(111) substrate. Intermolecular interactions are the main driving force for this ordering, resulting in a herringbone-like packing on the surface.

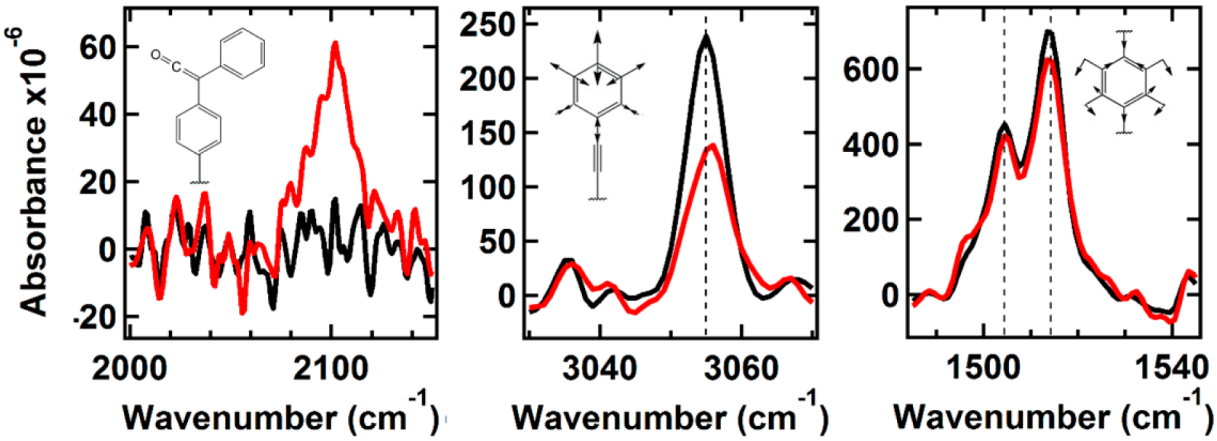

Figure 3. RAIRS spectra of monolayer before (black) and after (red) exposure of ~8 × 10^{15} O(^{3}P)/cm^2. New mode associated with ketenyl stretching appears at 2102 cm^{-1} (left), consistent with expected position of a biphenylketene-like moiety. Peak associated with C—H stretching mode of the phenyl ring at the vacuum/film interface (middle) decreases significantly upon exposure of the monolayer to O(^{3}P). Other peaks, such as the C═C semicircle stretching modes (right), remain unchanged at this level of exposure, suggesting that initial exposure results in formation of ketenes, resulting in canting of planes of interfacial phenyl rings toward the substrate, with the rest of the molecular backbone remaining intact.

molecules relative to the surface normal was not quantitatively characterized in this study; however, the most intense peaks observed correspond to modes with transition dipole moments parallel to the molecular axis. This is consistent with the oPE molecules being anchored with their molecular axes nearly perpendicular to the substrate, which is expected, since SAMs composed of these and similar oligophenylene molecules have been reported to exhibit small tilt angles relative to the surface normal.[28,30,36−39]

STM images of the pristine oPE-SAM are shown in Figure 2. The oPE molecules form highly ordered domains composed of two distinct close-packed structures: (1) a $(\sqrt{3} \times 2\sqrt{3})$R30° structure commensurate with the underlying Au(111) surface, containing lattice constants of a = 5.0 Å and b = 9.7 Å and observed by Dhirani et al.[29] and (2) an incommensurate structure with a rectangular lattice of a = 5.5 Å and b = 8.0 Å observed by Yang et al.[30] While both of these domains coexist on the surface and are shown in Figure 1B, we observe ~75% of the monolayer is composed of the incommensurate structure under our preparation conditions. Additionally, this structure remains constant throughout a bias voltage range of ±1 V.

The close-packed oPE molecules are bonded to the underlying Au(111) through the sulfur atom, with the molecular chain standing near-perpendicular to the surface (Figure 2C). Adjacent molecules are rotated to maximize $\pi-\pi$ interactions between the benzene substituent on neighboring chains, forming a herringbone-styled array of molecules across the domain. The face of the benzene rings located on the same molecular chain are aligned within the same plane and locked into this position by the triple bonds between the carbon atoms; this results in a different structure than SAMs composed of biphenylthiolate molecules, in which the orientation of the benzenes are independent from one another and are rotated with respect to each other on the same molecule to minimize steric effects.[40]

The rectangular unit cell is composed of oPE molecules that appear as both bright and dark features in the STM image. Yang et. al proposed that the difference in apparent STM height is the result of a change in the electronic structure between oPE molecules bound at different Au(111) lattice sites;[30] however, replicating the unit cell across a bulk-terminated Au(111) surface does not result in consistent binding locations for a given feature (i.e., not all "bright" molecules bind at the same Au(111) lattice site). More recently, a number of experimental groups have revealed the presence of gold adatoms at the interface of bulk-terminated Au(111) and thiol-based SAMs.[41−45] While STM is unable to image the gold/monolayer interface directly, changes in relative electronic structure across the monolayer surface is detectable, and we believe the rectangular unit cell with bright and dark features is the result

dx.doi.org/10.1021/jp504466r | J. Phys. Chem. C 2014, 118, 15846−15852

of a complex interfacial structure involving bulk-terminated Au(111), gold adatoms, and oPE molecules. Further study of oPE-SAM formation is needed to fully explain this observation.

DISCUSSION

Mechanism of O(^{3}P)/oPE-SAM Reaction. Upon exposure to O(^{3}P), distinct structural changes in the SAM are observed. These changes are summarized in Figure 3. The most notable is the appearance of a new mode at 2102 cm^{-1} immediately upon exposure of oPE-SAM to O(^{3}P). The peak position is consistent with formation of a ketene and closely matches that of the C═C═O stretching mode of biphenylketene at 2094 cm^{-1}.[46] Moreover, this is consistent with an expected product of electrophilic addition of O(^{3}P) onto an alkyne bond in oPE. Combined, these observations are congruent with a biphenylketene-like product being formed. In the gas phase, a phenyl shift occurring after addition onto biphenylacetylene results in a highly vibrationally excited triplet ketene, which cleaves to form CO and a carbene. On the thermally equilibrated surface, however, the excess energy from the reaction can dissipate through the SAM matrix. Additionally, the triplet biradical intermediate is likely stabilized on the surface to the singlet ketene, similar to collisional stabilization by surrounding inert gases in high-pressure gas reactions. While we can make no spectroscopic distinction between the two alkyne bonds of oPE, the argument can nevertheless be made that the alkyne bond closest to the vacuum/film interface is initially the most accessible.

Formation of a nonlinear ketene structure at the vacuum/film interface would naturally result in the canting of the interfacial benzene, given that the other end of the molecule is anchored to the substrate. Concurrent with the appearance of the ketene mode, exposure results in significant decay of the phenyl C−H peak at 3055 cm^{-1} alone; this change is not reciprocated in the rest of the IR signals of oPE-SAM. We assign this peak to the C−H stretching mode (20a) of the monosubstituted benzene of oPE located at the vacuum/film interface.[47] Decay of the 20a mode is attributed to a change in orientation of the phenyl ring plane—and therefore the orientation of the 20a transition dipole moment (TDM)—relative to the surface normal. The decrease supports canting of the ring, resulting in the 20a TDM ending up more parallel to the surface plane. Because of the surface selection rule of RAIRS, the intensity appears smaller because of the decrease in the magnitude of the perpendicular component of the 20a TDM even though the structure is still on the surface. The parallel component is "invisible", since the image dipole induced by the gold surface is equal in magnitude but opposite in direction, effectively canceling it out.

It is important to address other possible causes for the decrease in C−H mode intensity. Abstraction of hydrogen atoms from the phenyl rings can be ruled out because of the associated high energetic barrier (~60 kJ/mol for benzene[47]). Because of the persistence of the rest of the modes, oxidation of sulfur headgroups leading to desorption of entire chains does not satisfactorily account for the observed decay. Were this the case, all modes belonging to oPE would decay to the same extent, but the modes associated with C═C semicircle stretches, for example, decay by only a few percent over this same exposure (Figure 3C). It is also worth noting that these changes in the SAM take place only when O(^{3}P) is present in the molecular beam. Control trials using a pure neon discharge or an O_2 gas source, seeded in either helium or neon, without the discharge resulted in no detectable change in the structure of the SAM over similar total exposures. We can thus conclude that the structural changes are directly attributable to the presence of O(^{3}P).

On the basis of the above observations, we are able to propose a mechanism for the reaction of O(^{3}P) with oPE-SAM, a schematic of which is detailed in Figure 4. Upon dosing

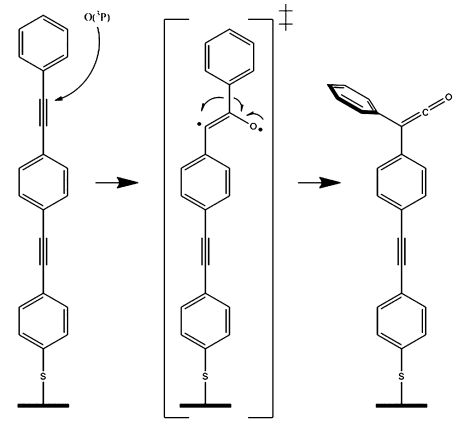

Figure 4. Proposed mechanism for O(^{3}P) reaction with oPE-SAM: electrophilic addition of O(^{3}P) onto the alkyne bonds closest to the vacuum/film interface results in formation of a triplet biradical intermediate that undergoes phenyl migration and is stabilized to singlet ketene by rapid equilibration with the SAM matrix.

O(^{3}P) onto oPE-SAM, the oxygen atoms react with the alkyne bond closest to the vacuum/film interface first to form a triplet biradical intermediate. This intermediate undergoes a phenyl shift to yield a vibrationally excited ketene that is stabilized on the surface to its singlet state, yielding a nonlinear biphenylketene-like moiety located at the vacuum/film interface. This reaction results in the canting of the molecular plane of the interfacial phenyl ring toward the substrate.

This mechanism is further corroborated by STM images of reacted oPE-SAM. The STM current, and therefore the "height" in an STM image, is a combination of both the electronic state and the topographic height; STM is not able to directly perform chemical analysis of individual molecules. Figure 5 shows a partially reacted oPE monolayer that contains areas of both reacted and unreacted molecules after ~3 × 10^{15} O(^{3}P)/cm^2 of exposure. We assign the bright molecules as

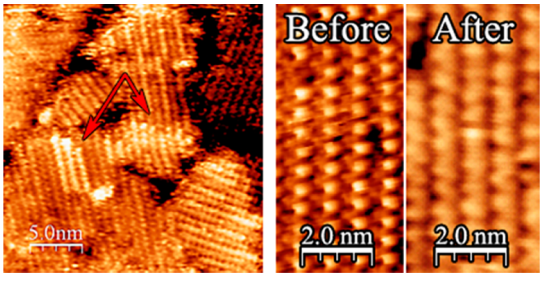

Figure 5. STM images (0.7 V, 40 pA) of oPE-SAM after exposure of ~3 × 10^{15} O(^{3}P)/cm^2 show that this reaction does not occur initially at domain boundaries but instead propagates along rows of the unit cell due to greater accessibility of nearby alkyne bonds after canting of the first interfacial phenyl ring. A rectangular lattice is conserved but with expanded dimensions (0.5 Å along each unit cell direction) to accommodate the newly formed nonlinear structures.

dx.doi.org/10.1021/jp504466r | J. Phys. Chem. C 2014, 118, 15846−15852

reacted oPE, based on an increased spacing of the lattice at these particular sites, while the darker molecules approximately retain the pristine lattice spacing. As observed in the RAIRS spectra, upon the formation of the ketene on a reacted molecule, the top benzene rotates downward and becomes more parallel to the gold surface. The reacted molecules appear brighter in the STM image despite the lower topographic height because of the change in the electronic structure upon the addition of the ketene and the resulting exposure of the benzene face. Neighboring unreacted oPE chains tilt and adjust to accommodate the wider reacted molecule, forcing the lattice to expand. Figure 5 also shows a direct comparison between the unreacted and reacted SAM, where the monolayer has maintained a rectangular unit cell and its lattice constants have expanded to a = 6.0 Å and b = 8.5 Å.

We observe in the STM images (Figure 5) that monolayer reactivity takes place at preferential sites. Interestingly, the reaction does not appear to occur initially at every molecule located along a domain boundary, where the triple bond would be the most exposed to the incident oxygen atoms, before propagating to molecules located in the interior of the domain. Instead, we observe that reacted molecules always appear along rows of the unit cell. After the reaction takes place at an initial molecule, the benzene rotates parallel to the gold surface, and the neighboring molecules expand slightly to accommodate the change in structure. This increases the accessibility of the triple bond on a neighboring molecule to additional oxygen atoms, propagating the reaction along a lattice direction and into the monolayer.

Finally, it is worth noting that continued exposure of oPE-SAM to O(^{3}P) results in severe disordering of the monolayer. All RAIRS peaks associated with oPE have significantly decayed in intensity by the time the monolayer has been exposed to ~50 × 10^{15} O(^{3}P)/cm^2. This is corroborated with STM images that display no molecular resolution at this level of exposure.

Kinetics of the O(^{3}P)/oPE-SAM Reaction. Appearance of the ketene mode, while reproducible, yields an IR signature that is weak in intensity. Additionally, ketenes formed may undergo further reaction with O(^{3}P) or O_2 as exposure continues. We have therefore monitored the kinetics of the reaction by characterizing the decay of the stronger 20a mode as a function of total exposure, detailed in Figure 6, which follows a first-order decay. As exposure increases, the intensity of this mode clearly does not approach zero, instead decaying to a value roughly 25% that of the original intensity. This observation agrees well with the proposed mechanism. Assuming the oPE chain is nearly perpendicular to the substrate, formation of the ketene results in the angle between surface normal and the 20a TDM increasing from ~0° to ~60°. This results in the magnitude of the perpendicular component of the TDM decreasing to roughly one-half its original value. Given intensity is proportional to the square of the magnitude of the TDM, the relative intensity of the 20a mode should be roughly one-fourth its initial value.

Taking into account the above points, we can assert that the total signal prior to exposure represents a fraction of remaining interfacial alkyne bonds of 100%. Additionally, the total signal as exposure approaches infinity approximates a remaining fraction of zero. At any point in between, the total 20a intensity is approximately a combination of these two values:

$$I_{tot} = I_{100\%}\theta + I_{0\%}(1 - \theta) \quad (1)$$

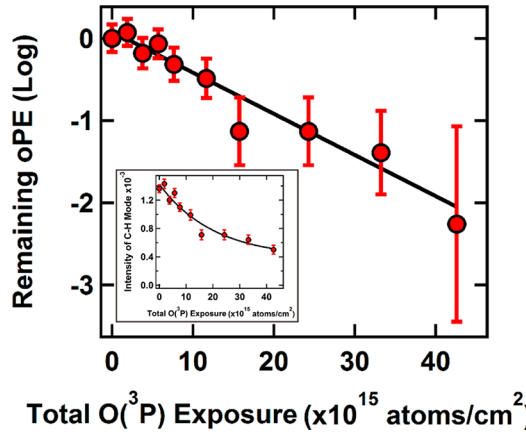

Figure 6. Plotting the log of remaining unreacted oPE versus total O(^{3}P) exposure yields a linear trend. Fitting the data to a Langmuirian model results in a reaction probability of 7 ± 2%. These data were derived from the decay of the C−H stretching mode intensity at 3055 cm^{-1} (inset), which tends toward ~25% of its original intensity given that the decay is a change in orientation of the interfacial phenyl ring relative to the substrate and not entire removal of the structure.

where θ is the aforementioned fraction; each data point can be converted to a remaining fraction. Plotting the natural log of this fraction versus the total O(^{3}P) exposure yields a linear decay, which fits well to a first-order Langmuirian model for the rate of O(^{3}P) addition onto the alkyne bond located closest to the vacuum/film interface. This allows for estimation of the initial reaction probability, γ_o:[48]

$$\ln \theta = -(\gamma_o/4A)\Phi \quad (2)$$

where Φ is the total exposure of O(^{3}P), and A is the average density of oPE molecules on the surface. A weighted linear least-squares fit to the data yields an initial reaction probability of 7 ± 2%. The average surface density, A, was estimated from the STM data, where the commensurate (~25%) and incommensurate (~75%) structure unit cells are calculated to contain 2 molecules per 44 ± 1 Å^2 and 48 ± 1 Å^2, respectively.

Use of the SAM as an ensemble of reactants provides a framework for controlling how reactants encounter each other in real space. The barrier for addition onto the alkyne bond of biphenylacetylene in the gas phase was measured by Eichholtz et al. to be 0.6 kJ/mol. Collisions between O(^{3}P) and oPE-SAM occur at the phenyl rings decorating the vacuum/film interface, where no reaction is observed to occur because of unfavorable energetics. Enforcing the majority of collisions to occur under unfavorable conditions yields a low reaction probability despite incident O(^{3}P) atoms having kinetic energies (9 kJ/mol) far above the energetic barrier. Only when incoming oxygen atoms penetrate the interface can they react with the underlying alkyne bonds.

The most readily accessible alkyne bonds in oPE-SAM are obscured from direct reaction by the interfacial phenyl rings, and so, the addition reaction would not be expected to follow Eley−Rideal kinetics and instead involve incorporation of O(^{3}P) into the SAM. Although gas/surface interactions utilizing oligophenylthiolate SAMs have not been explicitly characterized in the literature, studies of these types of interactions with n-alkanethiolate SAMs are plentiful. It is established that lateral motion in these SAMs effectively dissipates energy from collisions of gaseous species.[11−13,49,50] Specifically, it has been suggested that, for O(^{3}P) collisions with

dx.doi.org/10.1021/jp504466r | J. Phys. Chem. C 2014, 118, 15846−15852

n-alkanethiol SAMs under conditions similar to those outlined in this study, physisorption onto the interface dominates—only ~27% of $O(^3P)$ penetrates the interface.[50] Therefore, it is readily apparent that the low reaction probability is a direct result of the change in accessibility of the alkyne bonds in the SAM versus the gas phase. This is also in line with the findings of Eichholtz et al., where the pre-exponential factor for addition onto the alkyne bond was measured to be nearly 2 orders of magnitude smaller than addition onto the phenyl ring.[15] Enforcing the majority of collisions to occur with the phenyl rings naturally yields a lower probability for the addition reaction. Thus, the ability to stereodynamically control a reaction is demonstrated herein, in this case by restricting the accessibility of a reactive group just below the immediate vacuum/film interface.

SUMMARY AND CONCLUSIONS

Utilizing a combination of in situ RAIRS and STM, we have characterized and confirmed the mechanism of the reaction of $O(^3P)$ with phenyl-substituted alkynes. In situ RAIRS indicates that decay of the phenyl mode at the vacuum/film interface is a result of ketene formation between the top two phenyl rings of oPE-SAM and subsequent canting of the phenyl moiety toward the substrate plane. Subsequent characterization of changes in local topology using STM completes the picture by establishing that the reaction propagates along rows of the unit cell due to increased accessibility of a neighboring triple bond after one oPE molecule reacts. Kinetic measurements support a mechanism that relies on incorporation of $O(^3P)$ into the SAM matrix in order for reaction to occur. Unfavorable geometric constraints imposed upon the approach of the reactants yield low initial reaction probability despite establishing sufficient energetics. Through direct observation of the ketene intermediate, the use of oPE-SAM as a scaffold for an ensemble of oriented reactants proves effective in facilitating rapid thermal equilibration and detection of products not readily observed in the gas phase.

A crucial next step is to utilize SAMs in this manner with reactive groups located directly at the vacuum/film interface. Approaching reactants prepared in a supersonic beam could undergo direct reactions exhibiting Eley–Rideal kinetics given that incoming reactants have translational energies near or above associated energetic barriers. SAMs can readily be prepared with interfacial reactive groups in different orientations with respect to the surface plane, providing a direct route to stereochemical control. This technique is effective for the elucidation of orientation-dependent kinetics, with the added ability to "collisionally stabilize" reactive intermediates not necessarily detectable under, as an example, crossed molecular beam techniques using high collision energies.

AUTHOR INFORMATION

Corresponding Author

*Phone: (773) 702-7193; e-mail: s-sibener@uchicago.edu.

Notes

The authors declare no competing financial interest.

ACKNOWLEDGMENTS

This work was supported by the National Science Foundation, award number CHE-0911424. Partial support from the NSF Materials Research Science and Engineering Center at the University of Chicago is also acknowledged, award number DMR-0820054.

REFERENCES

(1) Polanyi, J. C. Some Concepts in Reaction Dynamics. *Acc. Chem. Res.* **1972**, *5*, 161–168.
(2) Bernstein, R. B. *Chemical Dynamics via Molecular Beam and Laser Techniques*; Clarendon Press: Gloucestershire, U.K., 1982.
(3) Levine, R. D.; Bernstein, R. B. *Molecular Reaction Dynamics and Chemical Reactivity*; Oxford University Press: Oxford, U.K., 1987.
(4) Moore, C. B.; Smith, I. M. W. Vibrational-Rotational Excitation: Chemical Reactions of Vibrationally Excited Molecules. *Faraday Discuss. Chem. Soc.* **1979**, *67*, 146–161.
(5) Orr-Ewing, A. J. Dynamical Stereochemistry of Bimolecular Reactions. *J. Chem. Soc. Faraday Trans.* **1996**, *92*, 881–890.
(6) Parker, D. H.; Bernstein, R. B. Oriented Molecular Beams via the Electrostatic Hexapole: Preparation, Characterization, and Reactive Scattering. *Annu. Rev. Phys. Chem.* **1989**, *40*, 561–595.
(7) Loesch, H. J. Orientation and Alignment in Reactive Beam Collisions: Recent Progress. *Annu. Rev. Phys. Chem.* **1995**, *46*, 555–594.
(8) Love, J. C.; Estroff, L. A.; Kriebel, J. K.; Nuzzo, R. G.; Whitesides, G. M. Self-Assembled Monolayers of Thiolates on Metals as a Form of Nanotechnology. *Chem. Rev.* **2005**, *105*, 1103–1169.
(9) Ulman, A. Formation and Structure of Self-Assembled Monolayers. *Chem. Rev.* **1996**, *96*, 1533–1554.
(10) Schreiber, F. Structure and Growth of Self-assembling Monolayers. *Prog. Surf. Sci.* **2000**, *65*, 151–256.
(11) Gibson, K. D.; Isa, N.; Sibener, S. J. Experiments and Simulations of Ar Scattering from an Ordered 1-Decanethiol/Au(111) Monolayer. *J. Chem. Phys.* **2003**, *119*, 13083–13095.
(12) Isa, N.; Gibson, K. D.; Yan, T.; Hase, W. L.; Sibener, S. J. Experimental and Simulation Study of Neon Collision Dynamics with a 1-Decanethiol Monolayer. *J. Chem. Phys.* **2003**, *120*, 2417–2433.
(13) Lu, J. W.; Day, B. S.; Fiegland, L. R.; Davis, E. D.; Alexander, W. A.; Troya, D.; Morris, J. R. Interfacial Energy Exchange and Reaction Dynamics in Collisions of Gases on Model Organic Surfaces. *Prog. Surf. Sci.* **2012**, *87*, 221–252.
(14) Sloane, T. M.; Brudzynski, R. J. Competition between Reactive Sites in the Reactions of Oxygen Atoms and Hydroxyl Radicals with Phenylacetylene and Styrene. *J. Am. Chem. Soc.* **1979**, *101*, 1495–1499.
(15) Eichholtz, M.; Kohl, S.; Schneider, A.; Vollmer, J.-T.; Wagner, H. G. The Reactions of $O(^3P)$ with Aromatic Hydrocarbons with Unsaturated Side Chains. *Symp. Int. Combust. Proc.* **1996**, *26*, 527–534.
(16) Kanofsky, J. R.; Lucas, D.; Pruss, F.; Gutman, D. Direct Identification of the Reactive Channels in the Reactions of Oxygen Atoms and Hydroxyl Radicals with Acetylene and Methylacetylene. *J. Phys. Chem.* **1974**, *78*, 311–316.
(17) Arrington, C. A., Jr.; Cox, D. J. Arrhenius Parameters for the Reaction of Oxygen Atoms, $O(^3P)$, with Propyne. *J. Phys. Chem.* **1975**, *79*, 2584–2586.
(18) Schmoltner, A. M.; Chu, P. M.; Lee, Y. T. Crossed Molecular Beam Study of the Reaction $O(^3P) + C_2H_2$. *J. Chem. Phys.* **1989**, *91*, 5365–5373.
(19) Harding, L. B. Theoretical Studies on the Reaction of Atomic Oxygen (^3P) with Acetylene. *J. Phys. Chem.* **1981**, *85*, 10–11.
(20) Harding, L. B.; Wagner, A. F. Theoretical Studies on the Reaction of Atomic Oxygen ($O(^3P)$) with Acetylene. 2. *J. Phys. Chem.* **1986**, *90*, 2974–2987.
(21) Xing, G.; Huang, X.; Wang, H.; Bersohn, R. Reactions of $O(^3P)$ with Alkynes: The CO and H Atom Channels. *J. Chem. Phys.* **1996**, *105*, 488–495.
(22) Girard, Y.; Chaquin, P. Addition Reactions of ^1D and ^3P Atomic Oxygen with Acetylene. Potential Energy Surfaces and Stability of the Primary Products. Is Oxirene Only a Triplet Molecule? A Theoretical Study. *J. Phys. Chem. A* **2003**, *107*, 10462–10470.

(23) Nguyen, T. H.; Vereecken, L.; Peeters, J. Quantum Chemical and Theoretical Kinetics Study of the $O(^3P)$ + C_2H_2 Reaction: A Multistate Process. *J. Phys. Chem. A* **2006**, *110*, 6696−6706.
(24) Schmoltner, A. M.; Chu, P. M.; Brudzynski, R. J.; Lee, Y. T. Crossed Molecular Beam Study of the Reaction $O(^3P)$ + C_2H_4. *J. Chem. Phys.* **1989**, *91*, 6926−6936.
(25) Casavecchia, P.; Capozza, G.; Segoloni, E.; Leonori, F.; Balucani, N.; Volpi, G. G. Dynamics of the $O(^3P)$ + C_2H_4 Reaction: Identification of Five Primary Product Channels (Vinoxy, Acetyl, Methyl, Methylene, and Ketene) and Branching Ratios by the Crossed Molecular Beam Technique with Soft Electron Ionization. *J. Phys. Chem. A* **2005**, *109*, 3527−3530.
(26) Haller, I.; Pimentel, G. C. Reaction of Oxygen Atoms with Acetylene to Form Ketene. *J. Am. Chem. Soc.* **1962**, *84*, 2855−2857.
(27) Gaedtke, H.; Glänzer, K.; Hippler, H.; Luther, K.; Troe, J. Addition Reactions of Oxygen Atoms at High Pressures. *Symp. Int. Combust. Proc.* **1979**, *14*, 295−303.
(28) Tour, J. M.; Jones, L., II; Pearson, D. L.; Lamba, J. J. S.; Burgin, T. P.; Whitesides, G. M.; Allara, D. L.; Parikh, A. N.; Atre, S. V. Self-Assembled Monolayers and Multilayers of Conjugated Thiols, α,ω-Dithiols, and Thioacetyl-Containing Adsorbates. Understanding Attachments between Potential Molecular Wires and Gold Surfaces. *J. Am. Chem. Soc.* **1995**, *117*, 9529−9534.
(29) Dhirani, A.-A.; Zehner, R. W.; Hsung, R. P.; Guyot-Sionnest, P.; Sita, L. R. Self-Assembly of Conjugated Molecular Rods: A High-Resolution STM Study. *J. Am. Chem. Soc.* **1996**, *118*, 3319−3320.
(30) Yang, G.; Qian, Y.; Engtrakul, C.; Sita, L. R.; Liu, G. Arenethiols Form Ordered and Incommensurate Self-Assembled Monolayers on Au(111) Surfaces. *J. Phys. Chem. B* **2000**, *104*, 9059−9062.
(31) Cai, L.; Yao, Y.; Yang, J.; Price, D. W., Jr.; Tour, J. M. Chemical and Potential-Assisted Assembly of Thioacetyl-Terminated Oligo-(phenylene ethynylene)s on Gold Surfaces. *Chem. Mater.* **2002**, *14*, 2905−2909.
(32) Béthencourt, M. I.; Srisombat, L.; Chinwangso, P.; Lee, T. R. SAMs on Gold Derived from the Direct Adsorption of Alkanethioacetates Are Inferior to Those Derived from the Direct Adsorption of Alkanethiols. *Langmuir* **2009**, *25*, 1265−1271.
(33) Singh, A.; Dahanayaka, D. H.; Biswas, A.; Bumm, L. A.; Halterman, R. L. Molecularly Ordered Decanethiolate Self-Assembled Monolayers on Au(111) from in Situ Cleaved Decanethiolate: An NMR and STM Study of the Efficacy of Reagents for Thioacetate Cleavage. *Langmuir* **2010**, *26*, 13221−13226.
(34) Sibener, S. J.; Buss, R. J.; Ng, C. Y.; Lee, Y. T. Development of a Supersonic $O(^3P_J)$, $O(^1D_2)$ Atomic Oxygen Nozzle Beam Source. *Rev. Sci. Instrum.* **1980**, *51*, 167−182.
(35) Greenler, R. G. Infrared Study of Adsorbed Molecules on Metal Surfaces by Reflection Techniques. *J. Chem. Phys.* **1966**, *44*, 310−315.
(36) Duan, L.; Garrett, S. J. An Investigation of Rigid *p*-Methylterphenyl Thiol Self-Assembled Monolayers on Au(111) Using Reflection-Absorption Infrared Spectroscopy and Scanning Tunneling Microscopy. *J. Phys. Chem. B* **2001**, *105*, 9812−9816.
(37) Ulman, A.; Kang, J. F.; Shnidman, Y.; Liao, S.; Jordan, R.; Choi, G.-Y.; Zaccaro, J.; Myerson, A. S.; Rafailovich, M.; Sokolov, J.; et al. Self-Assembled Monolayers of Rigid Thiols. *Rev. Mol. Biotechnol.* **2000**, *74*, 175−188.
(38) Dunbar, T. D.; Cygan, M. T.; Bumm, L. A.; McCarty, G. S.; Burgin, T. P.; Reinerth, W. A.; Jones, L., II; Jackiw, J. J.; Tour, J. M.; Weiss, P. S.; et al. Combined Scanning Tunneling Microscopy and Infrared Spectroscopic Characterization of Mixed Surface Assemblies of Linear Conjugated Guest Molecules in Host Alkanethiolate Monolayers on Gold. *J. Phys. Chem. B* **2000**, *104*, 4880−4893.
(39) Kang, J. F.; Ulman, A.; Liao, S.; Jordan, R.; Yang, G.; Liu, G. Self-Assembled Rigid Monolayers of 4′-Substituted-4-mercaptobiphenyls on Gold and Silver Surfaces. *Langmuir* **2001**, *17*, 95−106.
(40) Matei, D. G.; Muzik, H.; Gölzhäuser, A.; Turchanin, A. Structural Investigation of 1,1′-Biphenyl-4-thiol Self-Assembled Monolayers on Au(111) by Scanning Tunneling Microscopy and Low-Energy Electron Diffraction. *Langmuir* **2012**, *28*, 13905−13911.
(41) Maksymovych, P.; Yates, J. T., Jr. Au Adatoms in Self-Assembly of Benzenethiol on the Au(111) Surface. *J. Am. Chem. Soc.* **2008**, *130*, 7518−7519.
(42) Maksymovych, O.; Voznyy, O.; Dougherty, D. B.; Sorescu, D. C.; Yates, J. T., Jr. Gold Adatom as a Key Structural Component in Self-assembled Monolayers of Organosulfur Molecules on Au(111). *Prog. Surf. Sci.* **2010**, *85*, 206−240.
(43) Kautz, N. A.; Kandel, S. A. Alkanethiol/Au(111) Self-Assembled Monolayers Contain Gold Adatoms: Scanning Tunneling Microscopy before and after Reaction with Atomic Hydrogen. *J. Am. Chem. Soc.* **2008**, *130*, 6908−6909.
(44) Kautz, N. A.; Kandel, S. A. Alkanethiol Monolayers Contain Gold Adatoms, and Adatom Coverage Is Independent of Chain Length. *J. Phys. Chem. C* **2009**, *113*, 19286−19291.
(45) Jobbins, M. M.; Raigoza, A. F.; Kandel, S. A. Adatoms at the Sulfur-Gold Interface in 1-Adamantanethiolate Monolayers, Studied Using Reaction with Hydrogen Atoms and Scanning Tunneling Microscopy. *J. Phys. Chem. C* **2011**, *115*, 25437−25441.
(46) Cerioni, G.; Plumitallo, A.; Frey, J.; Rappoport, Z. Oxygen-17 and Carbon-13 NMR Studies of Diarylketenes. *Magn. Reson. Chem.* **1995**, *33*, 669−673.
(47) Barry, N. J.; Fletcher, I. W.; Whitehead, J. C. The Dynamics of OH Production in the Reaction $O(^3P)$ + Benzene. *J. Phys. Chem.* **1986**, *90*, 4911−4912.
(48) Lu, J. W.; Fiegland, L. R.; Davis, E. D.; Alexander, W. A.; Wagner, A.; Gandour, R. D.; Morris, J. R. Initial Reaction Probability and Dynamics of Ozone Collisions with a Vinyl-Terminated Self-Assembled Monolayer. *J. Phys. Chem. C* **2011**, *115*, 25343−25350.
(49) Yan, T.; Isa, N.; Gibson, K. D.; Sibener, S. J.; Hase, W. L. Role of Surface Intramolecular Dynamics in the Efficiency of Energy Transfer in Ne-Atom Collisions with a *n*-Hexylthiolate Self-Assembled Monolayer. *J. Phys. Chem. A* **2003**, *107*, 10600−10607.
(50) Tasić, U. S.; Yan, T.; Hase, W. L. Dynamics of Energy Transfer in Collisions of $O(^3P)$ Atoms with a 1-Decanethiol Self-Assembled Monolayer Surface. *J. Phys. Chem. B* **2006**, *110*, 11863−11877.